Effects of turbulence-mediated larval behavior on larval supply and settlement in tidal currents

Heidi L. Fuchs,[1] *Michael G. Neubert, and Lauren S. Mullineaux*
Woods Hole Oceanographic Institution, Woods Hole, Massachusetts 02543

Abstract

Intertidal gastropod larvae retract their vela and sink in strong turbulence, and this behavior potentially increases settlement in turbulent coastal habitats. We incorporated turbulence-induced sinking behavior of mud snail larvae (*Ilyanassa obsoleta*) in a vertical advection–diffusion model to characterize behavioral effects on larval supply and settlement in a tidal channel. Throughout flood and ebb tides, larvae that sink in turbulence have higher near-bed concentrations than passive larvae. This high supply of larvae enables behaving larvae to settle more successfully than passive larvae in strong currents characteristic of tidal inlets. Unlike passive larvae, those that sink in turbulence settle more successfully in stronger currents than in weaker ones and would concentrate their settlement in energetic tidal zones. Turbulence-mediated behavior may give intertidal larvae a greater ability to select habitats and may reduce larval mortality rates due to settlement failure.

Larvae of the intertidal mud snail *Ilyanassa obsoleta* have three distinct behaviors in the laboratory: upward-swimming, hovering, and sinking with retracted vela (Fuchs et al. 2004). The proportion of sinking larvae increases with the turbulence dissipation rate ε, resulting in a shift of the average larval velocity from upward to downward at ε ≈ 10^{-1} cm² s⁻³ (Fuchs et al. 2004).

In fact, many gastropod larvae sink in turbulence (e.g., Barile et al. 1994; Young 1995); one hypothesis is that they do so to avoid predators (Young 1995). Swimming predators such as krill, herring, and anchovies generate turbulence with dissipation rates estimated on the order of 10^{-1} cm² s⁻³ (Huntley and Zhou 2004). Sinking in turbulence at or above this level could be an escape mechanism for larvae that have no other defenses. Predators and prey also have higher contact rates in turbulence (e.g., McKenzie and Leggett 1991), and sinking to calmer water could reduce larval encounters with predators. Alternatively, if predators such as fish larvae also sink in turbulence, then both predators and prey could become more concentrated in calmer water where predators feed more efficiently, resulting in higher predation rates (Franks 2001).

A second hypothesis, one that we explore here, is that larvae of coastal gastropods use turbulence as an indicator of potentially suitable habitats and sink to reach the bottom and test the substrate (Chia et al. 1981; Fuchs et al. 2004). Larvae are most likely to encounter strong turbulence in the nearshore, and this hydrodynamic signal could indicate a proximity to energetic, shallow habitats. High turbulence dissipation rates (≥10^{-1} cm² s⁻³) are uncommon in shelf regions or open ocean (e.g., Dillon and Caldwell 1980; Oakey and Elliott 1982) but are typical of coastal areas and tidal inlets (e.g., Gross and Nowell 1985; George et al. 1994). Sinking in strong nearshore turbulence could increase the supply of larvae to the energetic coastal environments where suitable adult habitats are found, allowing more larvae to settle successfully.

To see whether the behavioral responses to turbulence that we measured in the laboratory (Fuchs et al. 2004) could affect settlement in situ, we constructed a vertical advection–diffusion model (e.g., Eckman 1990; Gross et al. 1992) whose output includes larval supply and settlement success. This advection–diffusion model allows us to express larval behavior as a population-average vertical velocity that varies with the turbulence dissipation rate, as we observed in the laboratory.

We restrict our attention to a typical mud snail habitat, a shallow tidal channel, and focus on temporal patterns of larval supply and settlement driven by tidal variation in turbulence. During peak flood and ebb tides, larvae that sink in turbulence are expected to have greater sinking fluxes than larvae with no response to turbulence. Therefore behaving larvae and passive larvae should concentrate near the bottom at different stages of the tidal cycle, potentially affecting settlement success. To settle, larvae must attach or burrow into the substrate, and their ability to do so is affected by time-dependent near-bed shear stresses (Crimaldi et al. 2002). During flood and ebb tides, when bed shear stress is above some critical value, sediment and larvae are transported as bedload or suspended load. When both the bed and the larvae are mobile, larval attachment to the bottom is less probable. Larvae might settle more easily during slack tides, but slack periods can be brief (~10 min, Ayers 1959). Temporal patterns of both larval supply and attachment probability

must be considered in evaluating whether turbulence-induced sinking could increase settlement success.

Several ecological terms have quantitative meanings in the models that follow. We define "larval supply" as the proportion of larvae that are within 1 cm of the bed. These larvae are within several body lengths of the bottom; they are likely to contact the substrate and are available for settlement. We define "settlement" as permanent attachment to the bottom; this definition is conventional (Scheltema 1974) and mathematically convenient. We define "settlement success" as the proportion of larvae that settle within one tidal cycle. One tidal cycle is the window of settlement opportunity for larvae that enter a tidal inlet on a flood tide and are flushed out on the subsequent ebb. We call those larvae that change their velocity in response to turbulence "behaving," and those with a constant velocity "passive."

Advection–diffusion model

The advection–diffusion equation is a useful spatially explicit model for the movement of organisms in environmental gradients. Advection–diffusion models have been used to describe settlement dynamics of passive larvae in steady currents over variable roughness elements (Eckman 1990) and of passive (Gross et al. 1992) and negatively phototactic (Eckman et al. 1994) larvae in tidal currents. Here, we develop an advection–diffusion model of larvae with turbulence-mediated behavior in a turbulent, tidal boundary layer.

The one-dimensional vertical advection–diffusion equation is shown in Eq. 1.

$$\frac{\partial C}{\partial t} = -\frac{\partial}{\partial z}\left(wC - K\frac{\partial C}{\partial z}\right) \qquad (1)$$

Its solution $C(z, t)$ is the concentration of larvae at height z and time t (*see Table 1* for symbols). Larvae are advected by their behavioral velocity $w(z, t)$ and diffused by the turbulent eddy diffusivity $K(z, t)$. We model larvae as passive (constant w) or with turbulence-dependent behavior, wherein w varies with the turbulence dissipation rate $\varepsilon(z, t)$ (described in *Behavioral parameters*). Both the dissipation rate and the eddy diffusivity K are functions of depth and a tidally oscillating shear velocity u_*, which is proportional to the free-stream velocity U_H (described in *Physical parameters*).

The larval concentration is also subject to the boundary conditions in Eq. 2.

$$-wC + K\frac{\partial C}{\partial z} = 0 \qquad \text{at } z = H$$
$$-wC + K\frac{\partial C}{\partial z} = -\Phi_s \qquad \text{at } z = 0 \qquad (2)$$

There is no flux at the surface ($z = H$) because larvae cannot leave through the air–water interface. A settlement flux Φ_s is specified at the bottom ($z = 0$) as in Eq. 3,

$$\Phi_s(t) = s(t)C(0, t) \qquad (3)$$

Table 1. List of symbols. Vertical velocities are positive upward.

Symbol	Description
C	Larval concentration
C_b/C_T	Larval supply
C_d	Drag coefficient
H	Water depth
K	Eddy diffusivity
Q	Settlement success
w	Population-averaged larval vertical velocity
s	Settlement velocity
$\bar{s}$	Time-averaged settlement velocity
T	Tidal period
t	Time
u_*	Shear velocity
$U_{H\infty}$	Maximum current velocity
z	Height above bottom
α_i	Proportion of larvae in behavioral mode i
ε	Turbulence dissipation rate
κ	von Karman's constant (=0.4)
μ_i	Mean velocity for behavioral mode i
Φ_s	Settlement flux

where $s(t)$ is a time-varying settlement velocity. We ignore the potential for substrate selection behavior and allow larvae to settle only when they contact the bottom. The settlement velocity is either zero, a constant, or a function of shear velocity (described in *Settlement success*).

We solved the system (Eqs. 1–3) numerically with the Matlab 6.5 partial differential equation (PDE) solver. This PDE solver discretizes the spatial components of the equation to generate an ordinary differential equation in time that is solved by numerical integration with a multi-step, implicit difference scheme (Matlab's ODE15s). We solved the equation on a linearly spaced grid of 0.1-cm depth increments from 0 to H with a uniform initial distribution ($C = 5$ larvae cm^{-3}) and saved the solutions every 100 s. With no settlement ($s(t) = 0$), the solution reaches a periodic steady state, with $C(z, t) = C(z, t + T)$, where T is a tidal period, after a time ranging from a few minutes to ~3.5 h, depending on the water depth, maximum current velocity, and behavior function. We expect the numerical spin-up times to be short because the physical mixing times ($\approx H^2/K$; Tennekes and Lumley 1972) are short for a shallow channel with high diffusivity (*see Physical parameters*). The model reached a periodic solution within 4 h for all conditions, so we started the model 4 h before slack tide and calculated larval supply (described in *Larval supply*) or settlement success (described in *Settlement success*) over one tidal cycle beginning at slack tide. We allowed no settlement during the spin-up time.

Physical parameters—Mud snails live primarily in soft-sediment intertidal areas, and this model was intended to simulate larval settlement in a shallow tidal channel. We use Barnstable Harbor, Massachusetts as a reference tidal inlet because this is a prime habitat for mud snails and the natal habitat of larvae used in Fuchs et al. (2004). We use water depths ($H = [1, 3, 5, 7]$ m) that are representative of the harbor at various locations and tidal stages, and three
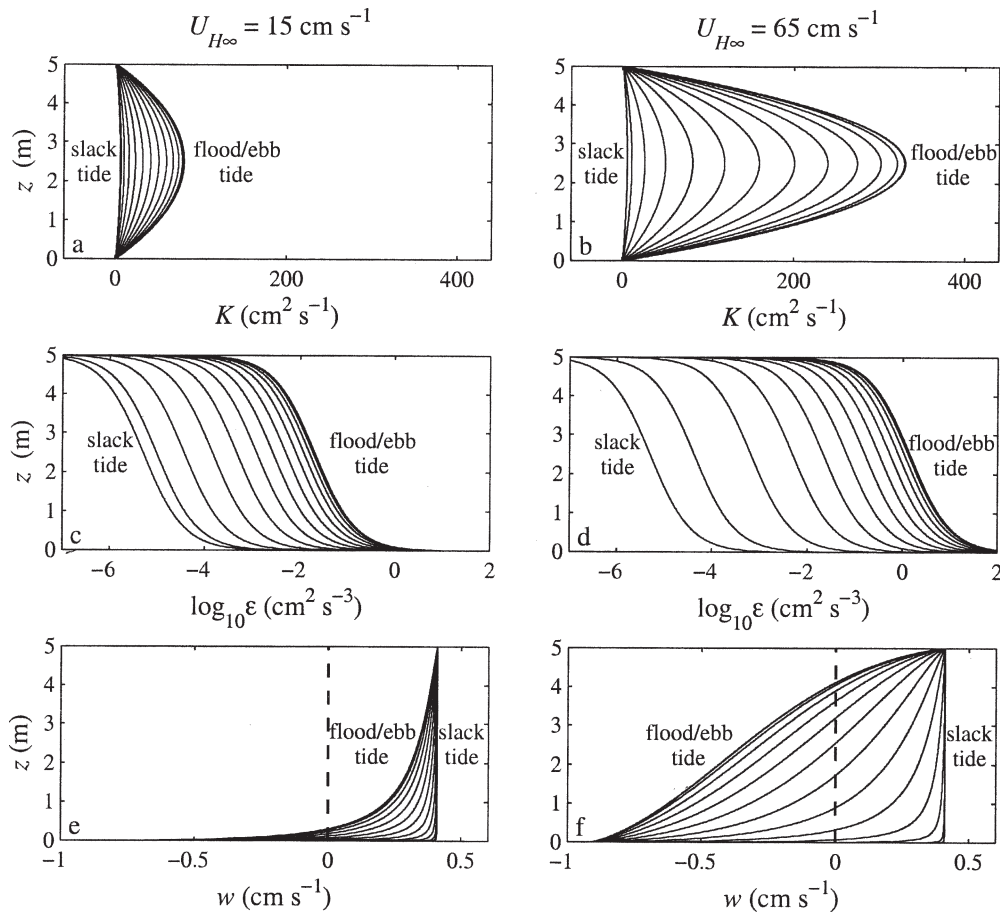
Fig. 1. Examples of modeled (a, b) eddy diffusivity K, (c, d) turbulence dissipation rate ε, and (e, f) larval velocity $w = f(\varepsilon)$ versus height above bottom z. Solid lines show 15-min intervals from slack tide to flood/ebb tide for $H = 5$ m and two maximum current speeds $U_{H\infty}$. Dashed vertical lines (panels e, f) indicate neutral buoyancy.

maximum current velocities ($U_{H\infty} = [15, 35, 65]$ cm s^{-1}). The fastest of these, $U_{H\infty} = 65$ cm s^{-1}, is representative of Barnstable Harbor (Ayers 1959), and the two slower current velocities might represent calmer, more sheltered estuaries. We assume the boundary layer to be depth-limited, as is the case at Barnstable Harbor under most conditions (Ayers 1959).

We model tides as symmetric, and the along-current free-stream velocity U_H varies periodically as

$$U_H(t) = 0.5U_{H\infty}\left(1 - \cos\frac{4\pi t}{T}\right) \qquad (4)$$

where T is a tidal period of 12.25 h. The free-stream velocity determines the shear velocity u_*, which ultimately defines the turbulence regime and influences larval settlement velocity. The shear velocity and the free-stream velocity are related by Eq. 5.

$$u_*(t) = \frac{U_H(t)}{10} \qquad (5)$$

This estimate is based on the nondimensional drag coefficient relationship $C_d = u_*^2/U_H^2$ (Gross and Nowell

1985). C_d is typically on the order of 3×10^{-3} for flow over smooth sandy substrates (Heathershaw 1979; Grant and Madsen 1986) but is $\sim 10^{-2}$ in Barnstable Harbor, probably because of form drag over large sandwaves (Fuchs et al. unpubl. data).

In our model, the vertical turbulent mixing is controlled by eddy diffusivity K. The eddy diffusivity is defined as the Reynolds stress divided by the vertical shear (Eq. 6).

$$K = -\overline{u'w'}\Big/\frac{\partial U}{\partial z} \qquad (6)$$

In steady channel flows, the Reynolds stress scales with shear velocity as $|\overline{u'w'}| = u_*^2(1 - z/H)$ (e.g., Nezu and Nakagawa 1993). The vertical shear near the boundary is given by the Law of the Wall as $\frac{\partial U}{\partial z} = u_*/\kappa z$, where $\kappa = 0.4$ is von Karman's constant. Thus K is

$$K = u_*\kappa z\left(1 - \frac{z}{H}\right) \qquad (7)$$

(Fig. 1a,b). We use this diffusivity form instead of the simpler equation $K = u_*\kappa z$ because Eq. 7 has a mid-depth

maximum on flood and ebb tides, as has been observed in well-mixed tidal channels (Sanford and Lien 1999; Rippeth et al. 2002). To prevent instabilities in our numerical model, we use

$$K = u_* \kappa z \left(1 - \frac{z}{H}\right) + 1 \text{ cm}^2 \text{ s}^{-1} \qquad (8)$$

so that K has a positive minimum. Although this minimum K is larger than the estimated pelagic diffusivity ($K \approx 0.1 \text{ cm}^2 \text{ s}^{-1}$, Munk and Wunsch 1998), $K = 1 \text{ cm}^2 \text{ s}^{-1}$ is on the order of minimum diffusivities measured over the continental shelf (e.g., Inall et al. 2000) and is a reasonable estimate of the background diffusivity in a shallow, unstratified channel.

Mud snail larvae have large sinking velocities, which could cause them to fall through eddies and be diffused less than the surrounding fluid (the "crossing trajectory" effect, Csanady 1963). For plankton with a constant velocity, it is possible to correct the diffusivity as $K_p = K_f(1 - \beta^2/\text{Pe}^2)$, where K_p is the particle diffusivity, K_f is the fluid diffusivity, β is a constant, and $\text{Pe} = wH/K_f$ is the Peclet number (O'Brien et al. 2003). In our model, however, behaving larvae have depth-dependent velocities (*see Behavioral parameters*; Fig. 1e,f) and $\partial K_p/\partial z$ can be discontinuous, which presents numerical difficulties. We are interested in settlement, so it is most important for the diffusivity to be correct at the bottom. Hinze (1975) suggested that no diffusivity correction is necessary if the particle velocity is less than the eddy characteristic velocity $w_c = (\varepsilon v)^{0.25}$, where $v = 0.01 \text{ cm}^2 \text{ s}^{-1}$ is the kinematic viscosity. Behaving larvae concentrate at the bottom only during flood and ebb tides (*see Larval supply*) when the dissipation rates and w_c are greatest. Thus for near-bottom larvae, the velocity ratio is generally $w/w_c \leq 1$, and the larval diffusivity approximates the fluid diffusivity where and when it matters most.

We model larval behavior as a function of the turbulence dissipation rate ε (*see Behavioral Parameters* section). Larvae must detect and respond to the smallest-scale eddies, which are characterized by the Kolmogorov length, time, and velocity scales. These smallest scales of turbulence are defined by ε (Tennekes and Lumley 1972). We assume the dissipation to be equal to the production of turbulent kinetic energy

$$\varepsilon = -\overline{u'w'} \frac{\partial U}{\partial z} \qquad (9)$$

(e.g., Trowbridge et al. 1999). According to the relationships given above, the dissipation rate is

$$\varepsilon = \frac{u_*^3}{\kappa z}\left(1 - \frac{z}{H}\right) \qquad (10)$$

(Fig. 1c,d). Equations 7 and 10 describe well the diffusivity and dissipation during flood and ebb tides in well-mixed tidal channels (e.g., Gross and Nowell 1985; Rippeth et al. 2002), including Barnstable Harbor (Fuchs et al. unpubl. data).

Behavioral parameters—We treat larvae as passive or as changing their behavior in response to turbulence. Passive

larvae have a constant velocity of $w = -0.05 \text{ cm s}^{-1}$ or $w = 0.05 \text{ cm s}^{-1}$, representing negative and positive buoyancy, respectively. These values are on the order of the vertical velocities reported for some bivalve and polychaete larvae (e.g., Cragg 1980; Butman et al. 1988; Jonsson et al. 1991).

We model behaving larvae as having three behavioral modes: (1) swimming, (2) hovering, and (3) sinking (e.g., see fig. 3a in Fuchs et al. 2004). The proportion α_i of larvae engaged in mode i depends on the turbulence dissipation rate, as determined by fitting the following functions to laboratory data (Fig. 2a–c) by logistic regression,

$$\begin{aligned} \alpha_1 &= f_1(\varepsilon) \\ \alpha_2 &= 1 - \alpha_1 - \alpha_3 \qquad (11) \\ \alpha_3 &= f_3(\varepsilon) \end{aligned}$$

where

$$f_i(\varepsilon) = \frac{1}{1 + exp(-b_{i0} - b_{i1} \log_{10} \varepsilon)} \qquad (12)$$

With ε in units of $\text{cm}^2 \text{ s}^{-3}$, the fitted parameters are $b_{10} = -0.96$, $b_{11} = -1.90$, $b_{30} = -0.44$, and $b_{31} = 1.71$. The population-average vertical velocity of larvae at a point z at time t is

$$w(z, t) = \sum_{i=1}^{3} \alpha_i(z, t)\mu_i \qquad (13)$$

where μ_i is the mean vertical velocity of larvae in mode i ($\mu_1 = 0.41 \text{ cm s}^{-1}$ for swimmers, $\mu_2 = -0.05 \text{ cm s}^{-1}$ for hoverers, and $\mu_3 = -0.92 \text{ cm s}^{-1}$ for sinkers). Note that the three behavioral modes are implicit in this larval velocity term $w(z, t)$, and the population-average larval velocity w is more negative at higher dissipation rates (Fig. 2d). As a result, larvae sink more near the bottom than near the surface, and sink more during flood and ebb tides than during slack tides (Fig. 1e,f).

Larval supply

We first characterized the effects of behavior on temporal patterns of larval supply by running the advection–diffusion model with no settlement ($\Phi_s = 0$). We calculated larval supply as the concentration in the bottom 1 cm normalized by the total number of larvae as in Eq. 14.

$$C_b(t)/C_T(t) = \frac{\int_0^1 C(z, t)dz}{\int_0^H C(z, t)dz} \qquad (14)$$

The magnitude and temporal pattern of larval supply are very different for passive larvae than for those with turbulence-dependent behavior (Fig. 3). For all current speeds, negatively buoyant larvae ($w = -0.05 \text{ cm s}^{-1}$) have large peaks in near-bed concentrations at slack tides. Positively buoyant larvae ($w = 0.05 \text{ cm s}^{-1}$) have low near-bed concentrations, but supply is higher during flood and ebb tides than during slack tides because turbulent mixing
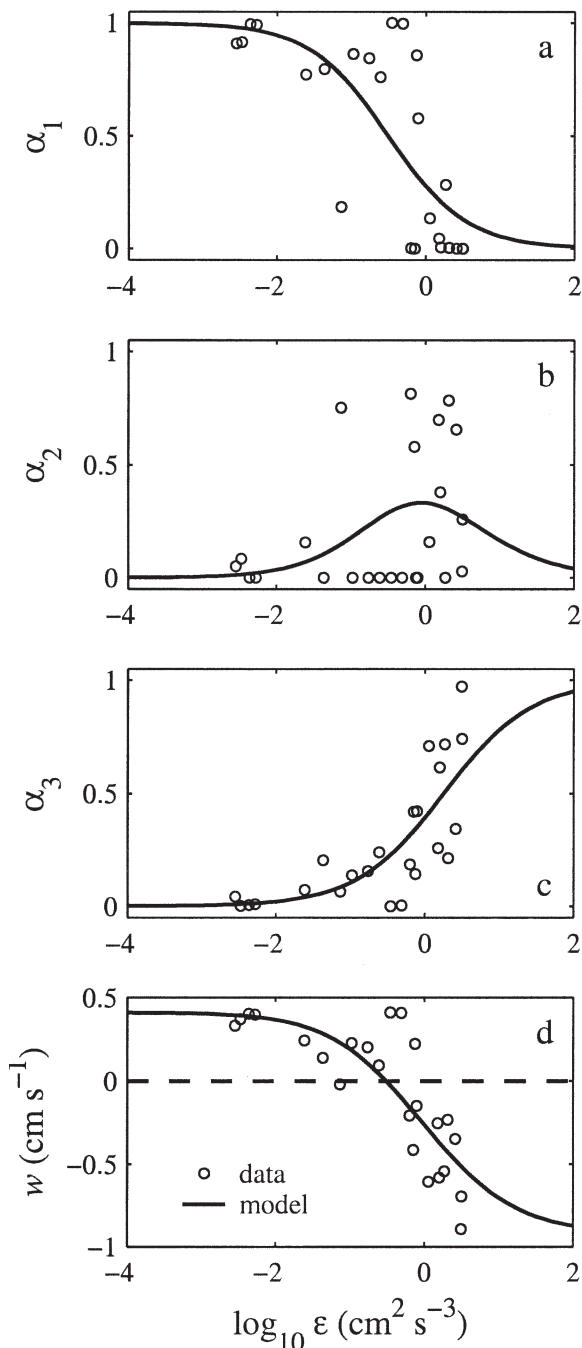
Fig. 2.   Proportions α_i of (a) swimming, (b) hovering, and (c) sinking larvae and (d) population-averaged larval vertical velocity w versus dissipation rate $\log_{10} \varepsilon$. Dashed line (panel d) indicates neutral buoyancy, circles are estimates from laboratory experiments (Fuchs et al. 2004), solid lines are forms used in the model.
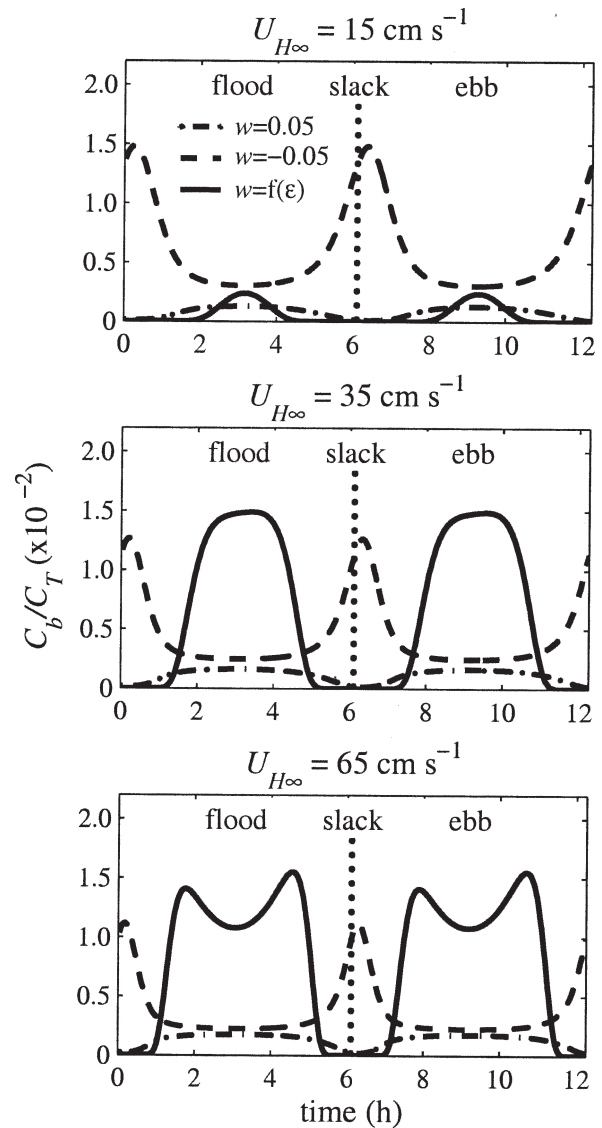

Fig. 3.   Larval supply C_b/C_T versus time for three values of $U_{H\infty}$. Near-bed larval concentrations C_b are normalized by the depth-integrated concentration C_T. $H = 5$ m. Dotted vertical line indicates slack tide, all other lines indicate behavior: $w = 0.05$ cm s^{-1}, dash-dot line; $w = -0.05$ cm s^{-1}, dashed line; $w = f(\varepsilon)$, solid line.

brings larvae down from the surface. The supply of positively and negatively buoyant larvae changes little with different maximum current velocities.

The supply of behaving larvae ($w = f(\varepsilon)$) to the bed is greatest during flood and ebb tides but is strongly dependent on the maximum current velocity (Fig. 3). For $U_{H\infty} = 15$ cm s^{-1}, the dissipation rate is always low enough that the larvae are swimming upward most of the time

(Fig. 1e) and the near-bed concentration is low. For $U_{H\infty} = 35$ cm s^{-1}, behaving larvae have broad peaks in near-bed concentration during flood/ebb tides. For $U_{H\infty} = 65$ cm s^{-1} these peaks are even broader, but larval supply is reduced slightly at peak flood and ebb tides as larvae are resuspended by intense turbulent mixing.

Under all flow conditions, turbulence-induced sinking behavior significantly affects the temporal patterns of larval supply to the bed. In moderate to strong currents, negatively-buoyant larvae have large peaks in near-bed concentration during slack tides, whereas behaving larvae are highly concentrated at the bed during flood and ebb tides. These opposite patterns of larval supply each could result in greater settlement success under different environmental conditions.

It might seem that larvae would settle more successfully by concentrating near the bottom during slack tides, when shear stress is low and sediments are stable. Yet as pointed out by Eckman et al. (1994), there is a cost to reaching the bottom during slack tide if the substrate is unsuitable for settlement. Larvae that reject substrates during slack tides have to wait for currents to increase and carry them away to potentially better sites. Larvae that concentrate near the bottom only during slack tides would have infrequent opportunities to settle and a lower overall probability of finding suitable substrates. In contrast, larvae that reach the bottom during flood and ebb tides could test substrates and be transported rapidly away from unsuitable sites. Larvae that concentrate near the bottom during most of the tidal cycle would have more frequent contact with the bottom and a higher overall probability of finding suitable substrates. Although negative buoyancy might be the best strategy if all substrates are suitable, turbulence-induced sinking is potentially a more successful strategy in patchy environments.

Settlement success

To explore how the timing of larval supply affects settlement success, we allowed larvae in contact with the bottom to attach and settle with a settlement velocity s. Once settled, larvae are unable to re-enter the water column. We used three settlement functions (Fig. 4), including two that depend on the tidally oscillating shear velocity,

$$
\begin{aligned}
\text{constant}: \quad & s(t) = c_1 \\
\text{linear}: \quad & s(t) = c_2[1 - u_*(t)/u_{*\max}] \\
\text{step}: \quad & s(t) = \begin{cases} 0.01 & \text{if } u_*(t) < u_{*\mathrm{cr}} \\ 0 & \text{if } u_*(t) \geq u_{*\mathrm{cr}} \end{cases}
\end{aligned}
\tag{15}
$$

where c_1 and c_2 are constants, $u_{*\max} = 0.1 U_{H\infty}$, and $u_{*\mathrm{cr}}$ is the critical shear velocity for bedload transport. We assume that $u_{*\mathrm{cr}}$ for mud snail larvae equals that of average Barnstable Harbor sediment (diameter $\approx 100~\mu$m; Scheltema 1961; Sanders et al. 1962), estimated from a Shields diagram to be $u_{*\mathrm{cr}} \approx 1.2$ cm s^{-1}. The linear and step cases are more realistic than a constant settlement velocity over a flat bottom, because larvae are expected to have more difficulty attaching to the bottom at higher shear velocities. The constant settlement velocity might be more appropriate over a rough bottom where there are low-shear areas between roughness elements.

We selected the constants c_1 and c_2 so that the settlement velocity averaged over a tidal cycle

$$
\bar{s} = \frac{1}{T} \int_0^T s(t)\,dt
\tag{16}
$$

is the same for the constant and linear function as for the step function. In the step function, larvae have a constant settlement velocity ($s = 0.01$ cm s^{-1}) when the shear velocity is below the critical value, and $\bar{s}$ is controlled by the duration of these settlement windows (Fig. 4). In the constant and linear functions, $\bar{s}$ determines the constant or
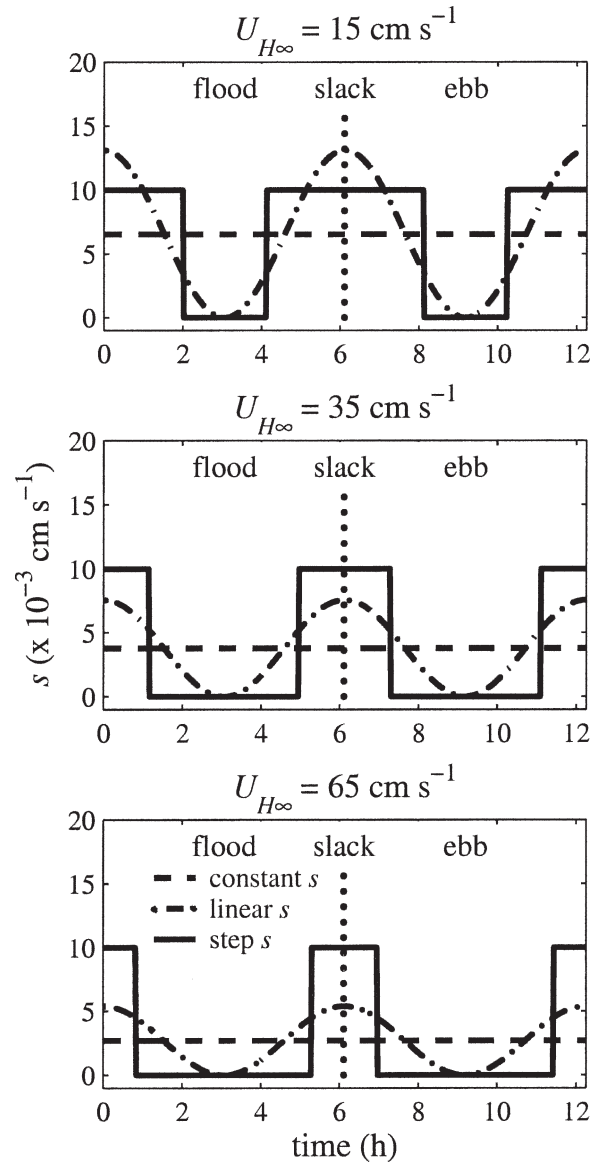

Fig. 4. Settlement velocities s versus time for three maximum current velocities $U_{H\infty}$. Dotted vertical line indicates slack tide; other lines indicate settlement function: constant s, dashed line; linear s, dash-dot line; step s, solid line.

maximum value of s. The time-averaged settlement velocity $\bar{s}$ is greatest at the smallest maximum current velocity ($\bar{s} = 0.0066$ cm s^{-1} at $U_{H\infty} = 15$ cm s^{-1}; $\bar{s} = 0.0038$ cm s^{-1} at $U_{H\infty} = 35$ cm s^{-1}; $\bar{s} = 0.0027$ cm s^{-1} at $U_{H\infty} = 65$ cm s^{-1}) because $u_*(t) < u_{*\mathrm{cr}}$ for longer time periods (Fig. 4). It is reasonable for the time-averaged settlement velocity to be greater in slower flows because slower flows are less likely to transport sediments and exert weaker drag forces on larvae as they are trying to settle.

We characterized settlement success Q as the proportion of larvae that settled within one tidal cycle,

$$
Q = 1 - \frac{\int_0^H C(z, T)\,dz}{\int_0^H C(z, 0)\,dz}
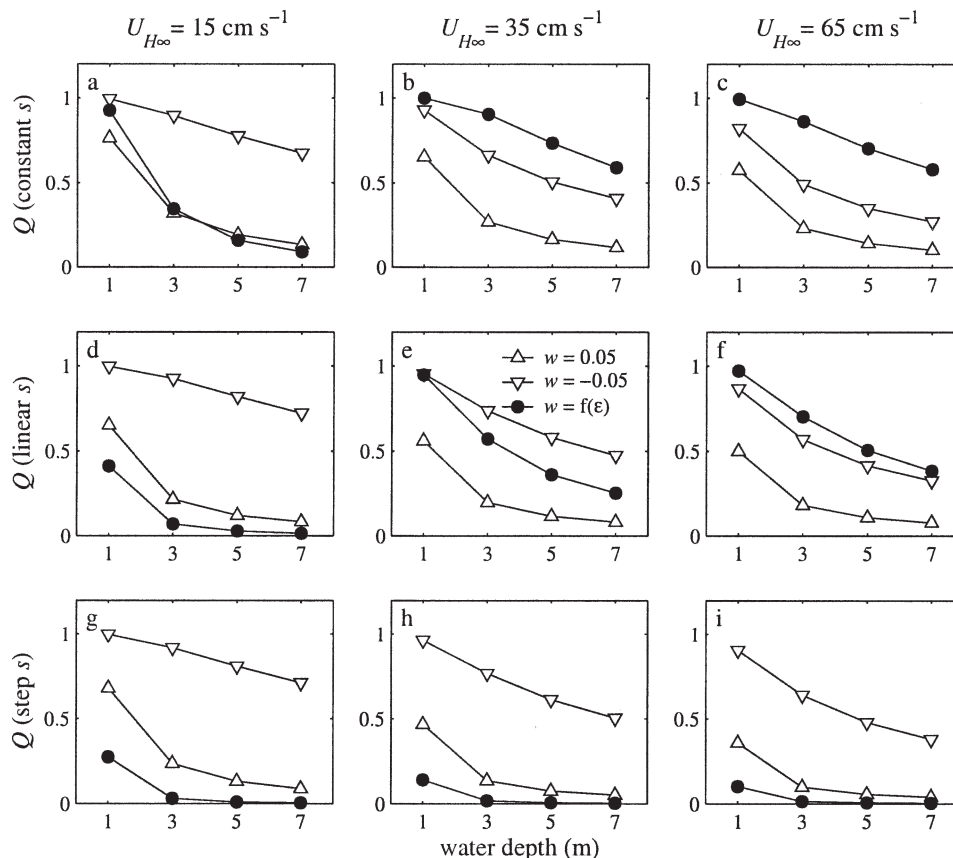\tag{17}
$$

Fig. 5.   Settlement success Q versus water depth H for three maximum current velocities $U_{H\infty}$ and three settlement velocity functions s. Symbols indicate behavior function: $w = 0.05$ cm s^{-1}, up-triangle; $w = -0.05$ cm s^{-1}, down-triangle; $w = f(\varepsilon)$, circle.

where $C(z, 0)$ is the initial concentration distribution. Larval settlement success ultimately depends on the combined effects of larval attachment probability, timing of larval contact with the bottom, and behavior.

We consider behavioral effects on settlement success in terms of two separate questions: (1) Under a given set of physical conditions, which behavior is most successful for settlement? and (2) For a given behavior, which physical conditions allow larvae to settle most successfully? We address these questions separately.

The most successful behavior for given conditions— Negative buoyancy always results in more settlement than positive buoyancy, but the relative benefits of turbulence-dependent behavior depend on both the settlement function s and the current regime (Fig. 5). For the constant settlement function, behaving larvae are less successful than negatively buoyant larvae in slow currents ($U_{H\infty} = 15$ cm s^{-1}) but are the best settlers in moderate and fast currents ($U_{H\infty} = 35$ and 65 cm s^{-1}; Fig. 5a–c). Likewise for the linear settlement function, behaving larvae are the least successful settlers in slow currents but the most successful settlers in fast currents (Fig. 5d–f). However, for the step settlement function, behaving larvae are always the least successful settlers (Fig. 5g–i) because their larval supply is near zero during settlement windows. The relative benefits

of different behaviors are fairly consistent with depth, suggesting that these results can be generalized for larvae settling in unstratified, shallow habitats.

Although the results in Fig. 5 might seem complicated, they are predictable on the basis of patterns of larval supply (Fig. 3) and settlement velocity (Fig. 4). The relative success of turbulence-mediated behavior depends almost entirely on whether peaks in larval supply are broad enough to coincide with periods of low bed shear stresses and moderate settlement velocities. Near-bed hydrodynamics are key to understanding whether turbulence-mediated behavior or passive transport is a better larval strategy for settlement. We return to this issue later.

The best settlement conditions for a given behavior— Passive larvae settle most successfully in the slowest currents ($U_{H\infty} = 15$ cm s^{-1}) regardless of whether they are positively or negatively buoyant and regardless of the settlement function (Fig. 6). It is intuitive that negatively buoyant larvae would settle more successfully in calm conditions, because in the absence of turbulent mixing they will sink to the bottom and have high larval supply. It is less obvious why positively buoyant larvae would settle more successfully in calm conditions, because in the absence of turbulent mixing they will float to the surface and have low larval supply. The explanation is that the
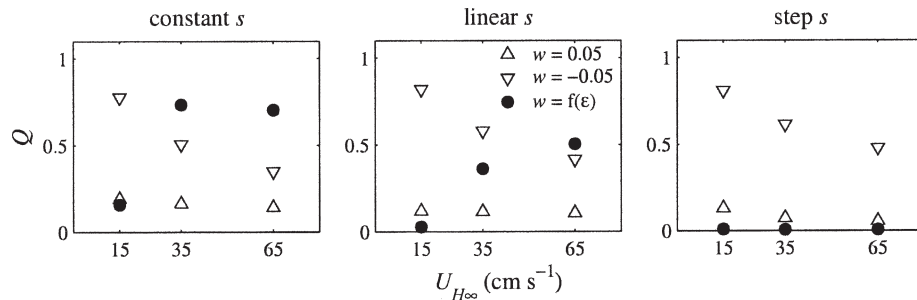
Fig. 6. Settlement success Q versus maximum current velocity $U_{H\infty}$ for three settlement velocity functions s at $H = 5$ m. Symbols indicate behavior function: $w = 0.05$ cm s^{-1}, up-triangle; $w = -0.05$ cm s^{-1}, down-triangle; $w = f(\varepsilon)$, circle.

supply of positively buoyant larvae is similarly low for all flow speeds (Fig. 3), but there is a higher time-averaged settlement velocity in slower flows (Fig. 4).

Unlike passive larvae, those with turbulence-dependent behavior settle most successfully in moderate ($U_{H\infty} = 35$ cm s^{-1}) or fast currents ($U_{H\infty} = 65$ cm s^{-1}) for the constant and linear settlement functions, respectively (Fig. 6). This result is interesting because the time-averaged settlement velocity $\bar{s}$ is actually lowest in the strongest currents (Fig. 4). The success of behaving larvae in moderate and fast currents indicates that extended periods of high larval supply can compensate for the lower settlement velocities expected in more turbulent environments. We conclude that turbulence-induced sinking would enhance larval settlement into energetic tidal zones.

Ecological consequences of turbulence-induced sinking

Our model allows some general predictions about where larvae are most likely to settle, given their behavior in the water column. Negatively buoyant larvae settle most successfully in slow to moderate currents. In contrast, larvae that sink in turbulence settle more successfully in more energetic currents. Thus for species that prefer calm, low-flow habitats, constant negative buoyancy is a good settlement strategy, but for intertidal species that inhabit turbulent inlets, sinking in turbulence would be a better settlement strategy. Mud snails are abundant in turbulent tidal channels, and our results strongly support the hypothesis that larval sinking in turbulence would enhance mud snail settlement in these energetic regions. Sinking in turbulence could be an adaptive response that enables larvae to settle actively into shallow, turbulent habitats.

We did not address the hypothesis that larvae sink to avoid predators, but there is no reason to believe that the two hypotheses are mutually exclusive. Predator-generated turbulence, distinctly nearshore turbulence, and the turbulence threshold for larval sinking all share an approximate lower limit of $\varepsilon \approx 10^{-1}$ cm^2 s^{-3}. Given this common turbulence threshold, we can reject neither the predator avoidance hypothesis nor the settlement hypothesis on the basis of observations of larval behavior. Our modeling results also prevent us from ruling out the possibility that

turbulence-induced sinking is a settlement behavior. For intertidal species, sinking in turbulence could increase larval survival in multiple ways. Larvae that sink in turbulence might escape being eaten by predators (but *see* Franks 2001) and could have lower mortality rates during dispersal. These larvae also are more likely to settle into suitable intertidal habitats than into unsuitable offshore habitats and should have lower mortality rates at or after settlement. This behavior could reduce larval wastage, both by increasing larval survival in the plankton and by increasing settlement success.

Model simplifications

Population-averaged larval behavior—Our advection–diffusion model simplifies the larval supply and settlement processes in several ways, including the expression of larval behavior as a population-averaged vertical velocity. To see whether stochastic, individual behaviors might significantly affect our results, we also constructed a stochastic particle-tracking model (Fuchs 2005). The advection–diffusion and particle-tracking models produced nearly identical larval concentrations over the interior of the spatial domain, but the particle-tracking model underestimated larval concentrations near the boundaries (top and bottom 1 cm). Ross and Sharples (2004) suggested two methods for correcting inaccuracies near the boundaries in particle-tracking models, but these corrections require manipulation of the near-boundary region and are problematic for settlement studies. It remains unclear whether we would learn anything more by modeling complex larval behaviors at the individual level. In our system, the turbulent diffusivities are very large relative to larval behavioral velocities, and more complicated individual behaviors are unlikely to affect larval supply unless they significantly alter the average larval velocity. We think that we have a good representation of the population-averaged larval response to turbulence because our behavior functions (Eqs. 11–13) are based on laboratory observations (Fig. 2). For the turbulent coastal zones we are interested in, we expect that multiple behaviors can be modeled implicitly as a population-averaged velocity with no loss of accuracy.

Boundary layer—We ignored two important boundary layer characteristics that probably would improve the

relative settlement success of behaving larvae. First, our model excludes turbulence intermittency at the bed. Even during flood and ebb tides, there are lulls between turbulent bursts at the bed, and the duration of these lulls can be estimated as $\sim 6H/U_{H\infty}$ (Nezu and Nakagawa 1993). At peak flood/ebb tides, the lulls would be on the order of ~ 10–70 s for the depths and current velocities used in this study. The shear stress is lower during lulls, and larvae could reasonably be expected to stick or burrow into sediments during some of these periods. Given this intermittency, the settlement condition imposed by our step function is overly strict. Behaving larvae that have high larval supply during flood/ebb tides probably are able to exploit the intermittent stress lulls for settlement.

Our second boundary layer simplification is the absence of roughness elements. Roughness elements influence the vertical diffusivity profile near the bed and the horizontal distribution of shear stress along the bottom. Although the roughness element spacing has complex effects on larval attachment probability (Crimaldi et al. 2002), larval settlement is generally greater over dense roughness elements than over flat beds (Eckman 1990). Flat beds are rare in tidal inlets such as Barnstable Harbor, where ripples and epifauna provide small-scale bottom topography. Mud snails themselves form dense aggregations with a roughness height of 1–2 cm, and their presence could alter the diffusivity and shear stress profiles to enhance settlement of larvae during flood/ebb tides where adult snails are present. This potential mechanism for gregarious settlement could be effective even in the absence of any specific larval response to the adult snails.

Behavior—Our models are behaviorally simple in that larvae respond only to turbulence, and interactions with the bed are ignored. Changes in behavior near the bed could increase both the supply of larvae and the attachment probability. Larvae near the bottom probably react to biochemical properties of the substrates (e.g., Hadfield and Koehl 2004), and might sink more readily when these substrates are attractive for settlement, increasing larval supply. Once larvae reach the bottom, the attachment probability is influenced by larval substrate selectivity (Scheltema 1961). If larvae fail to attach to suitable substrates because of high shear stress, they might gain settlement opportunities by tumbling along the bottom as bedload (e.g., Jonsson et al. 1991; Pawlik and Butman 1993). Other behaviors, such as burrowing into sediments, could raise the shear velocity at which larvae are eroded and thus increase the settlement velocity. These larval interactions with the bed would help larvae find good substrates over small spatial scales; in contrast, sinking in turbulence would help intertidal larvae settle into suitable habitat regions.

We suspect that the settlement consequences of different behaviors ultimately depend on the spatial scales of habitat patchiness. Patchy qualities include the suitability of substrates as well as temporal and spatial variability in bed shear stress. The relationship between habitat patchiness, behavior, and settlement success was beyond the scope of this paper but will be addressed with a two-dimensional model in a future study.

References

AYERS, J. C. 1959. The hydrography of Barnstable Harbor, Massachusetts. Limnol. Oceanogr. **4:** 448–462.

BARILE, P. J., A. W. STONER, AND C. M. YOUNG. 1994. Phototaxis and vertical migration of the queen conch (*Strombus gigas* Linne) veliger larvae. J. Exp. Mar. Biol. Ecol. **183:** 147–162.

BUTMAN, C. A., J. P. GRASSLE, AND E. J. BUSKEY. 1988. Horizontal swimming and gravitational sinking of *Capitella* sp. I (Annelida: Polychaeta) larvae: Implications for settlement. Ophelia **29:** 43–57.

CHIA, F. S., R. KOSS, AND L. R. BICKELL. 1981. Fine structural study of the statocysts in the veliger larva of the nudibranch, *Rostanga pulchra*. Cell Tissue Res. **214:** 67–80.

CRAGG, S. M. 1980. Swimming behaviour of the larvae of *Pecten maximus* (L.) (Bivalvia). J. Mar. Biol. Assoc. UK **60:** 551–564.

CRIMALDI, J. P., J. K. THOMPSON, J. H. ROSMAN, R. J. LOWE, AND J. R. KOSEFF. 2002. Hydrodynamics of larval settlement: The influence of turbulent stress events at potential recruitment sites. Limnol. Oceanogr. **47:** 1137–1151.

CSANADY, G. T. 1963. Turbulent diffusion of heavy particles in the atmosphere. J. Atmos. Sci. **20:** 201–208.

DILLON, T. M., AND D. R. CALDWELL. 1980. The Batchelor spectrum and dissipation in the upper ocean. J. Geophys. Res. **85:** 1910–1916.

ECKMAN, J. E. 1990. A model of passive settlement by planktonic larvae onto bottoms of differing roughness. Limnol. Oceanogr. **35:** 887–901.

———, F. E. WERNER, AND T. F. GROSS. 1994. Modelling some effects of behavior on larval settlement in a turbulent boundary layer. Deep-Sea Res. II **41:** 185–208.

FRANKS, P. J. S. 2001. Turbulence avoidance: An alternate explanation of turbulence-enhanced ingestion rates in the field. Limnol. Oceanogr. **46:** 959–963.

FUCHS, H. L. 2005. Biophysical coupling between turbulence, larval behavior, and larval supply. Ph.D. thesis. Massachusetts Institute of Technology and Woods Hole Oceanographic Institution.

———, L. S. MULLINEAUX, AND A. R. SOLOW. 2004. Sinking behavior of gastropod larvae (*Ilyanassa obsoleta*) in turbulence. Limnol. Oceanogr. **49:** 1937–1948.

GEORGE, R., R. E. FLICK, AND R. T. GUZA. 1994. Observations of turbulence in the surf zone. J. Geophys. Res. **99:** 801–810.

GRANT, W. D., AND O. S. MADSEN. 1986. The continental-shelf bottom boundary layer. Ann. Rev. Fluid Mech. **18:** 265–305.

GROSS, T. F., AND A. R. M. NOWELL. 1985. Spectral scaling in a tidal boundary layer. J. Phys. Oceanogr. **15:** 496–508.

———, F. E. WERNER, AND J. E. ECKMAN. 1992. Numerical modeling of larval settlement in turbulent bottom boundary layers. J. Mar. Res. **50:** 611–642.

HADFIELD, M., AND M. A. R. KOEHL. 2004. Rapid behavioral responses of an invertebrate larva to dissolved settlement cue. Biol. Bull. **207:** 28–43.

HEATHERSHAW, A. D. 1979. The turbulent structure of the bottom boundary layer in a tidal current. Geophys. J. R. Astr. Soc. **58:** 395–430.

HINZE, J. O. 1975. Turbulence. McGraw-Hill.

HUNTLEY, M. E., AND M. ZHOU. 2004. Influence of animals on turbulence in the sea. Mar. Ecol. Prog. Ser. **273:** 65–79.

INALL, M. E., T. P. RIPPETH, AND T. J. SHERWIN. 2000. Impact of nonlinear waves on the dissipation of internal tidal energy at a shelf break. J. Geophys. Res. **105:** 8687–8705.

JONSSON, P. R., C. ANDRÉ, AND M. LINDEGARTH. 1991. Swimming behaviour of marine bivalve larvae in a flume boundary-layer flow: Evidence for near-bottom confinement. Mar. Ecol. Prog. Ser. **79:** 67–76.

MCKENZIE, B. R., AND W. C. LEGGETT. 1991. Quantifying the contribution of small-scale turbulence to the encounter rates between larval fish and their zooplankton prey: Effects of wind and tide. Mar. Ecol. Prog. Ser. **73:** 149–160.

MUNK, W., AND C. WUNSCH. 1998. Abyssal recipes II: Energetics of tidal and wind mixing. Deep-Sea Res. I **45:** 1977–2010.

NEZU, I., AND H. NAKAGAWA. 1993. Turbulence in open-channel flows. A. A. Balkema.

OAKEY, N. S., AND J. A. ELLIOTT. 1982. Dissipation within the surface mixed layer. J. Phys. Oceanogr. **12:** 171–185.

O'BRIEN, K. R., G. N. IVEY, D. P. HAMILTON, A. M. WAITE, AND P. M. VISSER. 2003. Simple mixing criteria for the growth of negatively buoyant phytoplankton. Limnol. Oceanogr. **48:** 1326–1337.

PAWLIK, J. P., AND C. A. BUTMAN. 1993. Settlement of a marine tube worm as a function of current velocity: Interacting effects of hydrodynamics and behavior. Limnol. Oceanogr. **38:** 1730–1740.

RIPPETH, T. P., E. WILLIAMS, AND J. H. SIMPSON. 2002. Reynolds stress and turbulent energy production in a tidal channel. J. Phys. Oceanogr. **32:** 1242–1251.

ROSS, O. N., AND J. SHARPLES. 2004. Recipe for 1-D Lagrangian particle tracking models in space-varying diffusivity. Limnol. Oceanogr. Methods **2:** 289–302.

SANDERS, H. L., E. M. GOUDSMIT, E. L. MILLS, AND G. E. HAMPSON. 1962. A study of the intertidal fauna of Barnstable Harbor, Massachusetts. Limnol. Oceanogr. **7:** 63–79.

SANFORD, T. B., AND R-C. LIEN. 1999. Turbulent properties in a homogeneous tidal bottom boundary layer. J. Geophys. Res. **104:** 1245–1257.

SCHELTEMA, R. S. 1961. Metamorphosis of the veliger larvae of *Nassarius obsoletus* (Gastropoda) in response to bottom sediment. Biol. Bull. **120:** 92–109.

———. 1974. Biological interactions determining larval settlement of marine invertebrates. Thalassia Jugoslavica **10:** 263–296.

TENNEKES, H., AND J. L. LUMLEY. 1972. A first course in turbulence. MIT Press.

TROWBRIDGE, J. H., W. R. GEYER, M. M. BOWEN, AND A. J. WILLIAMS III. 1999. Near-bottom turbulence measurements in a partially mixed estuary: Turbulent energy balance, velocity structure, and along-channel momentum balance. J. Phys. Oceanogr. **29:** 3056–3072.

YOUNG, C. M. 1995. Behavior and locomotion during the dispersal phase of larval life, p. 249–278. *In* L. McEdward [ed.], Ecology of marine invertebrate larvae. CRC.